A conserved arginine near the filter of Kir1.1 controls Rb/K selectivity

Henry Sackin[1,*], **Mikheil Nanazashvili**[1], **Hui Li**[1], **Lawrence G. Palmer**[3], and **D. Eric Walters**[2]

[1]Dept. of Physiology & Biophysics, The Chicago Medical School; RFU, IL USA

[2]Dept. of Biochemistry, The Chicago Medical School; RFU, IL USA

[3]Dept of Physiology & Biophysics; Weill Medical College of Cornell University; New York, NY USA

Abstract

ROMK (Kir1.1) channels are important for K secretion and recycling in the collecting duct, connecting tubule and thick ascending limb of the mammalian nephron. We have identified a highly conserved *Arg* in the P loop of the channel near the selectivity filter that controls Rb/K selectivity. Mutation of this *Arg* to a *Tyr* (R128Y-Kir1.1b, R147Y-Kir1.1a) increased the macroscopic conductance ratio, G_{Rb}/G_K by 17 ± 3 fold and altered the selectivity sequence from $NH_4 > K > Tl > Rb \gg Cs$ in wt-Kir1.1 to: $Rb > Cs > Tl > NH_4 \gg K$ in R128Y, without significant change in the high K/Na permeability ratio of Kir1.1. R128M produced similar, but smaller, increases in Rb, Tl, NH_4 and Cs conductance relative to K. R128Y remained susceptible to block by both external Ba and the honeybee toxin, TPNQ, although R128Y had a reduced affinity for TPNQ, relative to wild-type. The effect of R128Y-Kir1.1b on the G_{Rb}/G_K ratio can be partly explained by a larger single-channel Rb conductance (12.4 ± 0.5 pS) than K conductance (<1.5 pS) in this mutant. The kinetics of R128Y gating at -120 mV with Rb as the permeantion were similar to those of wt-Kir1.1 conducting Rb, but with a longer open time (129 ms vs. 6 ms for wt) and two closed states (13 ms, 905 ms), resulting in an open probability (Po) of 0.5, compared to a Po of 0.9 for wt-Kir1.1, which had a single closed state of 1 ms at -120 mV. single-channel R128Y rectification was eliminated in excised, inside-out patches with symmetrical Rb solutions. The large increase in the Rb/K conductance ratio, with no change in K/Na permeability or rectification, is consistent with R128Y-Kir1.1b causing a subtle change in the selectivity filter, perhaps by disruption of an intra-subunit salt bridge (R128-e118) near the filter.

Keywords

rubidium; K; channel; ROMK; C-type; inactivation

Introduction

The better than 100 to 1 selectivity of potassium channels for K over Na is often attributed to a tight fit between dehydrated K ions and the main chain carbonyl oxygens of the selectivity filter.[1] In this model, the high selectivity for K over Na is a consequence of size-constrained ion binding sites within a structurally constrained filter.[2-4] However, the energetic preference for K over Na may not absolutely require a rigid filter structure since molecular dynamic calculations indicate that a flexible, dynamic filter can also produce a highly selective channel.[5,6]

Correspondence to: Henry Sackin; henry.sackin@rosalindfranklin.edu.

In addition, salt bridges adjacent to the selectivity filter may also affect the cation selectivity of K channels in ways that are not fully understood. For example, modification of a P-loop salt bridge (E138R-R148E) abolished the K/Na preference of the strong inward rectifier Kir2.1.[7] On the other hand, the E71-D80 bridge near the selectivity filter of KcsA did not alter ion selectivity.[8]

Since previous studies indicated that mutation of the conserved *Arg* (R148-Kir2.1) to *Lys, His, Cys* or *Glu* produced nonconducting membrane channels,[7] we were somewhat surprised that two mutations of the homologous *Arg* (R128Y, R128M) in Kir1.1b produced robust inward Rb currents. Consequently, we examined how these two *Arg* mutants (R128Y, R128M-Kir1.1b) altered cation selectivity in Kir1.1 and whether this was in any way related to disruption of a conserved salt bridge (E118-R128-Kir1.1b, homologous to E138-R148-Kir2.1) in the P loop, near the selectivity filter.

Replacement of the *Arg* at R128-Kir1.1b by either a *Tyr* or *Met* markedly increased the conductance of Rb, Tl, NH_4 and Cs relative to K, without significant changes in the K to Na permeability ratio. This suggests that subtle changes in the region near the filter can alter the cation selectivity of Kir1.1 inward rectifiers, without affecting the high K/Na permeability of these channels.

Results

Macroscopic selectivity and permeability

Oocytes expressing wt-Kir1.1b were bathed in either 100 mM external KCl or 100 mM external RbCl. Results obtained on the same oocyte (Fig. 1) indicated that inward wt-Kir1.1 Rb conductance was 0.7 ± 0.1 times as large as inward K conductance; outward conductances were not significantly different, consistent with outward K current being independent of the external cation.

In contrast, oocytes expressing R128Y-Kir1.1b had an inward Rb conductance (green circles, Fig. 2) that was 12 fold larger than their inward K conductance (black squares, Fig. 2). R128Y whole-cell outward conductance was similar whether the external solution was K or Rb, consistent with outward current being carried by K and with R128Y having a low outward K conductance (Fig. 2).

Although the I-V curves for K and Rb intersected the origin for wt-Kir1.1 (Fig. 1), the I-V relation for R128Y-Kir1.1b did not pass through the origin when the bath contained 100 mM external Rb (green circles, Fig. 2). The apparent reversal potential of -35 mV for Rb permeation through R128Y in 100 mM Rb solutions may indicate systematic block of inward Rb current by high internal oocyte K.

Average inward and outward conductances were also determined in uninjected oocytes bathed in 100 mM K solutions (magenta curve, Fig. 2). Since the endogenous inward conductance of uninjected oocytes (4.5 ± 1 μS) was small compared to R128Y inward K conductance, we judged it to be a negligible source of error in our conductance ratio calculations (Table 1).

We also estimated the inward Na conductance of R128Y-Kir1.1b by measuring whole-cell oocyte currents in 100 mM NaCl without K, Rb, Cs, Tl or NH_4. Under these conditions, inward whole-cell conductance averaged 2.3 ± 1 μS (not significantly different from uninjected oocytes); whereas outward current was similar to the K outward currents of Figure 2 (green circles, $0 < V < 200$ mV). These results are consistent with R128Y having a very low inward G_{Na}/G_{Rb} similar to wt-Kir1.1.

In addition to its effect on relative Rb/K conductance, the R128Y mutation also dramatically increased the ratio of Cs/K inward conductance (Fig. 4). This increase in cesium conductance was particularly striking since cesium normally functions as a blocking ion in wt-Kir1.1b, which has only a slight inward Cs current at very high (-200 mV) intracellular potentials (Fig. 3). In contrast, R128Y-Kir1.1b exhibits a sizable inward Cs current in 100 mM CsCl, at oocyte potentials more negative than -120 mV (Fig. 4). The small outward K current originating from the oocyte was largely unaffected by the presence of 100 mM external Cs and was similar to the outward K current of Figure 2.

We also investigated the conductance of other cations relative to K in both R128Y and R128M. These data on Rb, Tl, NH_4 and Cs inward conductances are summarized in Table 1. As indicated in the first row, wt-Kir1.1b had a cation selectivity sequence: K > NH_4 = Tl > Rb ≫ Cs, consistent with previous results.[15]

In contrast, the cation selectivity sequence for R128Y-Kir1.1b was: Rb > Cs > NH_4 > Tl > K. The R128Y mutation increased G_{Rb}/G_K by 17 fold and increased G_{Cs}/G_K by 43 fold. Whole-cell selectivity sequences, derived from macroscopic currents, implicitly include information about open probability as well as channel conductance and are therefore not necessarily equivalent to single-channel selectivity sequences (discussed later). Finally, replacing the *Arg* at R128 with *Met* had a similar (but smaller) effect on relative Rb/K conductance, where the selectivity sequence for R128M was: NH_4 > Rb > Tl > Cs > K (Table 1).

Since we were initially concerned that the R128Y mutation was simply rendering Kir1.1 non-selective to cations by disrupting the filter, we specifically examined the cation/Na permeability ratios by measuring reversal potential shifts in: wt-Kir1.1b, R128Y and R128M oocytes during isosmolar replacements of Na by: K, Rb, Tl or NH_4. A subset of these results are shown in Figure 5, where reversal potentials for R128Y are plotted as a logarithmic function of K, Rb, Tl or NH_4. Although wt-Kir1.1 is characterized by similar inward and outward currents for both K and Rb (Fig. 1), R128Y-Kir1.1b has markedly different inward and outward currents (Fig. 2). Consequently, we estimated the R128Y reversal potentials for Rb, Tl and NH_4 by extrapolation of the inward currents to zero current on the abscissa (inset, Fig. 5). These values may be more negative than the true reversal potential due to curvature of the I-V relationship.

A complete set of cation permeability ratios were obtained by simultaneously fitting all permeability ratios (Eqs 1–3) to all the reversal potential data from wt-Kir1.1b, R128Y and R128M during isosmolar replacements of external Na by: K, Rb, Tl or NH_4. These are summarized in Table 2. However for clarity, only the reversal potential data for R128Y-Kir1.1b are shown in Figure 5. The logarithmic dependence of potential on cation concentration (Fig. 5) indicates that the GHK Eqs (1–3) constitute a relatively good model, even for multi-ion pore inward rectifiers.

Two general statements can be made about the global permeability ratio fitting results (Table 2). First of all, replacement of R128 by *Tyr* or *Met* did not diminish the normally large preference for K over Na that characterizes channels of the Kir family. Second, there was no significant effect of either R128Y or R128M on each individual cation permeability ratio (columns, Table 2). These results are in marked contrast to the large effect of these mutations on relative conductance (Table 1).

Interaction between K and Rb in the pore of R128Y

Interactions between K and Rb were investigated in R128Y oocytes at the macroscopic current level. Inward conductance was found to be a saturable function of K in KCl

solutions (no Rb) and a saturable function of Rb in RbCl solutions (no K), as indicated by the average data in Figure 6. We modeled this interaction using a single saturable binding site for K and Rb. Although in reality the permeation process involves multiple binding sites and energy barriers, the simpler model was sufficient to describe the basic observed features with a minimum of free parameters and in our view is more instructive than more complex schemes. The parameters for a simplified single-site competitive inhibitor model (Eq 4, Methods) were fit to the data of Figure 6, where $K_K = 22 \pm 4$ mM and $K_{Rb} = 11 \pm 2$ mM and maximal conductances were $G_{Rbmax} = 1.3 \pm 0.2 \times 10^{-3}$ S and $G_{Kmax} = 0.3 \pm 0.03 \times 10^{-3}$ S.

As indicated by the family of curves in Figure 6, progressive addition of K to external Rb solutions proportionately decreased normalized inward Rb conductance (ordinate), where the inhibitory effect of external K saturated at concentrations greater than 100 mM. In the context of an enzyme model (Eq 4, Methods), the data of Figure 6 imply that K reduces Rb currents by acting as a partial agonist with a lower maximal conductance. However, the finding that this model becomes less accurate at high K concentrations suggests that ion-ion interactions within the permeation pathway should ultimately be included in a full description of the Kir multi-ion pore.

R128Y affects external toxin block but not internal pH gating

Mutation of R128-Kir1.1b diminished external block of Kir1.1 by the modified honeybee toxin, TPNQ. In wt-Kir1.1, the toxin TPNQ binds and blocks the outer mouth of the channel, dependent on external pH; with pKa ranging from 7×10^{-11} M at $pH_o = 6$ to 8×10^{-9} M at $pH_o = 8$. TPNQ also blocked R128Y-Kir1.1b, although at a significantly reduced affinity (Fig. 7). The K_D for TPNQ block of R128Y remained pH-dependent, but R128Y was more resistant to TPNQ block than wt-Kir1.1, with half maximal block varying from 1.7×10^{-8} M at $pH_o = 6$ to 4×10^{-6} M at $pH_o = 8$.

Presumably, TPNQ blocks the Kir1.1 family by plugging the outer vestibule of the K channel pore with its alpha-helical portion.[16] The similarity of TPNQ block in both wt-Kir1.1 and R128Y suggests that R128Y produces only minor changes in the conformation of the outer mouth of the channel. Nonetheless, these were sufficient to alter the affinity of TPNQ binding (and block).

R128Y-Kir1.1b inward Rb current was completely blocked by 5 mM external Ba, similar to wt-Kir1.1. Differences in the K_D for Ba block between wt and R128Y were not determined in these studies.

In contrast to TPNQ block at the extracellular mouth of the channel, there was no effect of R128Y on pH gating (Fig. 8). Both wt-Kir1.1b (ROMK) and R128Y had similar pKa's during progressive internal acidification, produced by permeant acetate buffers (Fig. 8). This is not surprising since R128 is structurally distant from both the presumed pH gate at the bundle crossing of inner transmembrane helices[11] as well as presumed cytoplasmic pH sensors. Neither wild-type nor R128Y were gated by changes in external pH alone when impermeant buffers were used.

Realkalization of R128Y oocytes restored channel activity within 30 min if the extracellular bath contained 100 mM Rb (black line, Fig. 8), but not if it contained 100 mM K (dashed red line, Fig. 8). Between 2 and 3 hours of alkalization were required for R128Y oocytes to recover their original channel activity in 100 mM external K solutions. This inactivation of R128Y in K solutions has been previously reported,[17] but its elimination by external Rb is a new observation and is consistent with the general finding that Rb is a preferred substrate for R128Y-Kir1.1b.

R128Y single-channel currents

Inward Rb currents through single R128Y channels were recorded at different patch potentials in the cell-attached mode (Fig. 9). The current-voltage relation was linear for inward Rb current (Fig. 10), but there was no evidence of outward current, which would be carried by K under these conditions. All cell-attached recordings were corrected for average oocyte potential determined as -45 ± 5 mV (n = 11) in separate, two-electrode voltage clamp experiments on similar batches of R128Y oocytes, bathed in 10 mM external K.

The average single-channel Rb conductance was 12.4 ± 0.5 pS (n = 16) in cell-attached R128Y patches with 100 mM Rb in the pipette. This is similar to the wt-Kir1.1 inward Rb conductance of 18 ± 2 pS, previously reported for wt-Kir1.1b oocytes in Rb (zero Mg) solutions.[15]

We could not detect convincing single-channel K currents through R128Y-Kir1.1b in either direction, which is not unexpected since the macroscopic G_K through R128Y was 12-fold smaller for K than Rb. This, together with the measured Rb single-channel conductance of 12.4 pS (above), suggests that the R128Y single channel K conductance could be about 1 pS, which is below the resolution of our recording system. This is in contrast to readily observed inward and outward K currents in wt-Kir1.1b cell-attached patches.[18]

Since the mutation (R128Y-Kir1.1b) is near the selectivity filter, R128Y might be expected to alter the fast kinetics of channel gating in addition to ion selectivity.[19] This was assessed by comparing the kinetics of Rb permeation through R128Y (Fig. 9) with wt-Kir1.1b Rb kinetics,[12] using patches containing only a single channel. At a membrane potential of $V_m = -120$ mV, R128Y-Rb currents had significantly longer open times (129 ms, Fig. 11A) than wt-Kir1.1b-Rb currents (6 ms).[20]

However, at this voltage (-120 mV), R128Y had a lower open probability (Po = 0.52), compared to wild-type (Po = 0.91). This was largely the result of R128Y having two closed states (Fig. 11B), of duration 13 ms (88%) and 905 ms (12%), both of which were significantly longer than the average 1 ms Rb closed state of wt-Kir1.1b.[12]

In addition, R128Y also exhibited a hyperpolarization-dependent decrease in both open probability (Fig. 12) and mean open-time (Fig. 13), similar to (but somewhat steeper than) the hyperpolarization dependent decrease seen with wt-Kir1.1b.[20] Mean closed times showed a more complicated dependence on membrane potential (Fig. 14).

Inward and outward currents through R128Y excised patches

The absence of obvious outward single-channel currents in R128Y cell-attached patches (Figs. 9 and 10) could in principle result either from R128Y having a strong inward rectification or a low K conductance, since outward current would be carried by K in cell-attached patches.

R128Y rectification was addressed by comparing inward and outward Rb currents in excised (inside-out) patches, with 100 mM RbCl solutions on both sides of the membrane (Fig. 15). Excised R128Y currents were similar to cell attached currents except that outward currents had more flickery kinetics, with shorter open and closed times than inward currents (Fig. 15).

The important point is that Rb current in R128Y excised patches was characterized by a linear I-V relation with no evidence of increased rectification, in the absence of Mg and polyamines (Fig. 16). On the average, the mean inward Rb conductance for R128Y excised

patches was 11.8 ± 0.6 pS (n = 10), which was similar to the mean inward Rb conductance of 12.4 ± 0.5 pS (n = 16) in R128Y cell-attached patches.

Cation dependence of single channel conductance

The cation dependence of single channel conductance was measured in cell attached patches on R128Y-Kir1.1b oocytes, bathed in 10 mM KCl and acetate buffers to control intracellular pH at 7.8. The pipette contained 100 mM concentrations of either K, Rb, Tl NH_4 or Cs, and results are summarized in Table 3.

Monovalent cation conductances were determined at membrane potentials between -100 mV and -200 mV, except for Cs whose conductance was measured between -150 mV and -250 mV. In general, R128Y had lower single-channel conductances than wt-Kir1.1b for: K, Rb, Tl and NH_4. However, the decrease in K and NH_4 single channel conductance was much greater than the decrease in Rb or Tl conductance produced by this mutation.

Discussion

R128Y increases Rb and Cs selectivity relative to K

Replacing a single highly conserved *Arg* residue in the P-loop near the selectivity filter of Kir1.1 (R128-Kir1.1b), by *Tyr* increased the macroscopic G_{Rb}/G_K conductance by 17 fold (Table 1), but did not significantly change either P_{Na}/P_K or P_{Rb}/P_K (Table 2). This implies that R128Y-Kir1.1b (and to a lesser extent R128M) increases Rb/K cation selectivity without completely disrupting the selectivity filter. Furthermore, this increase in Rb/K appears to result, in large part, from a selective decrease in K conductance.

The R128Y mutation also profoundly affected the Cs conductance of the channel. Normally, wt-Kir1.1 has a very low Cs conductance (Fig. 3), with external Cs acting as a voltage dependent blocker for K permeation.[21] However, R128Y-Kir1.1b displayed a sizable inward Cs current at membrane potentials more negative than -120 mV (Fig. 4).

Both R128Y and R128M produced similar increases in G_{Tl}/G_K and G_{NH4}/G_K, but R128Y produced a much larger increase in both G_{Rb}/G_K and G_{Cs}/G_K than did R128M (Table 1). In theory, R128Y and R128M should be equally effective at breaking the intra-inter subunit salt-bridge at E118-R128-E132-Kir1.1b.[17] However, the greater increase in both G_{Rb}/G_K and G_{Cs}/G_K with R128Y compared to R128M implies that salt bridge disruption cannot be the sole cause of the increased Rb/K selectivity.

In contrast to their effect on conductance ratios, both R128Y and R128M had relatively minor effects on the cation permeability ratios (Table 2). This would imply similar equilibrium energetics for Rb and K binding to the pore and a similar energy well depth for both Rb and K in wt-Kir1.1, R128Y and R128M. On the other hand, the low macroscopic and single-channel K conductance of R128Y suggests that this mutation establishes a higher energy barrier for K somewhere in the permeation path, probably within the selectivity filter.

In K free solutions, Rb permeation through R128Y was a saturable function of external Rb concentration (green curve, Fig. 6), consistent with occupancy of one|or more binding sites within the permeation pathway. Although the K conductance of R128Y is low, K is nonetheless an effective blocker of Rb permeation through R128Y, suggesting that both K and Rb probably bind to at least some of the same sites in the selectivity filter.

Previous failure to detect functional channels with R148 mutants of Kir2.1, despite evidence of membrane expression,[7] could be explained by altered cation selectivity in which *Arg* mutants of Kir channels conduct Rb much better than K.

Single channel recordings confirm an increase in Rb/K conductance ratio

In wild-type Kir1.1 (line 1, Table 3), Rb single-channel conductance (18 pS) was 60% of the K single-channel conductance (33 pS), consistent with macroscopic G_{Rb} being 70% of macroscopic G_K (line 1, Table 1). This correspondence implies a similar P_o for Rb and K permeation through wt-Kir1.1.

Attempts to record single-channel inward K currents through cell-attached R128Y patches did not yield convincing single-channel conductances greater than 1.5 pS (the lower limit of our recording system). Hence, the single-channel K conductance of R128Y is most likely less than 1.5 pS in 100 mM K solutions.

Since R128Y-Kir1.1b had similar single-channel kinetics with Rb, NH_4 and Cs, we can estimate the single-channel g_K of R128Y by dividing the single-channel Rb, NH_4 and Cs conductances (Table 3) by their respective macroscopic conductance ratios (Table 1). Thallium gave somewhat more flickery kinetics, similar to previous results with wt-Kir1.1,[15] and was not used in these estimates.

Applying the above algorithm to the Rb, NH_4 and Cs data of Tables 1 and 3, the estimated single-channel K conductance for R128Y was: 1.1pS (12.4 pS/11.7) using G_{Rb}/G_K, 1.6 pS (8.2 pS/5.1) using G_{NH4}/G_K, and 1.4 pS (11.8 pS/8.6) using G_{Cs}/G_K. Again, these estimates for g_K (R128Y) assume similar P_o for K, Rb, NH_4 and Cs permeation through R128Y, which appears to be the case.

Based on the single-channel conductances of Table 3, we can make the general statement that R128Y altered the conductance sequence from: $NH_4 > K > Tl > Rb \gg Cs$ for wild-type to: $Rb > Cs > Tl > NH_4 \gg K$ for R128Y. This is similar to the selectivity sequence observed with macroscopic currents through R128Y: $Rb > Cs > NH_4 > Tl \gg K$, reinforcing the assumption that macroscopic conductances reflect single channel conductances in this mutant.

The largest decrease in single-channel conductance occurred for K, the ion with the smallest Pauling diameter (2.66 Å). Sodium, which has an even smaller diameter than K, had its permeability reduced proportionately by R128Y, such that P_{Na}/P_K remained low (0.007). On the other hand, ions whose Pauling diameters were somewhat larger than K (i.e., Tl = 2.8 Å, Rb = 2.96 Å, NH_4 = 3.0 Å and Cs = 3.4 Å) showed less decrease in single channel conductance with R128Y. Cs even exhibited a large increase in single channel conductance. This raises the possibility that replacement of the *Arg* side-chain by a *Tyr* (R128Y) altered the selectivity filter to energetically accommodate monovalent cations of slightly larger diameter. In the Eisenman formalism the conductance selectivity sequence changes from type IV to type II, suggesting a weaker electric field strength.[22]

R128Y rectification

We examined the effect of R128Y-Kir1.1b on rectification at the single-channel level in excised inside-out patches with 100 mM RbCl on both sides of the membrane. The R128Y excised single-channel I-V relation was essentially linear with an inward Rb conductance of 11.8 ± 0.6 pS (n = 10), and had no obvious signs of rectification in the absence of Mg and polyamines (Fig. 16). This is similar to what was observed in excised (Mg free) patches on wt-Kir1.1.

The presence of clear outward Rb currents from R128Y (Figs. 15 and 16) argues that the apparent rectification of macroscopic R128Y currents (Fig. 2) results from R128Y having a very low outward K conductance relative to its high inward Rb conductance, and not from R128Y having different rectification than wt-Kir1.1b.

R128Y alters gating kinetics

In patches having only a single channel, the kinetics of inward Rb current (Fig. 9) were qualitatively similar to previously determined Rb kinetics through wt-Kir1.1. However, R128Y had longer open times (129 ms vs. 6 ms for wt) and two closed states (13 ms, 905 ms), yielding an average open probability (Po) of 0.5 at -120 mV, compared to a Po > 0.9 for wt-Kir1.1, which had a single closed state of 1 ms for Rb permeation.[12] In addition, the hyperpolarization-dependent decrease in Po for inward Rb current was larger with R128Y (Fig. 12) than with wt-Kir1.1.[12]

Previous studies had indicated that the fast flickery gating and voltage dependent kinetics of wt-Kir1.1 could be partly explained by permeant ion block of the channel at the selectivity filter.[19] The present results are consistent with this interpretation if it is assumed that R128Y produces only a subtle conformational change that affects the fast kinetics and cation selectivity at the filter, without altering the global structure of the channel.

R128Y and wt-Kir1.1 have similar pH gating

As shown in Figure 8, R128Y-Kir1.1b had no significant effect on Kir1.1 pH gating, which presumably occurs at the bundle-crossing of inner transmembrane helices.[11] This confirms that the R128Y mutation does not alter the large scale structure of the channel or produce long range allosteric changes in the transmembrane helices.

Although K current through R128Y was substantially less than Rb current, a pKa could be readily determined from normalized pH titrations for both K and Rb (Fig. 8). The pKa's for the two cations were quite similar in R128Y and were similar to the pKa for K permeation through wt-Kir1.1.[23]

As previously reported, R128Y whole-cell K conductance inactivated during acidification in 100 mM K solutions (dashed red line, Fig. 8) and only recovered between 2 and 3 hours after realkalization.[17] However, in the present study, we found that 100 mM external Rb prevented this pH inactivation such that R128Y conductance returned rapidly to its original value after realkalization (black line, Fig. 8).

This effect of 100 mM Rb (compared to K) on blocking R128Y inactivation is consistent with Rb being more effective than K at keeping the R128Y selectivity filter from collapsing since it enters the filter region more readily than K.

R128Y modifies external binding of TPNQ

The effect of R128Y on TPNQ block is also consistent with our hypothesis that R128Y produces a subtle conformational change at the outer mouth of the channel. Previous studies had indicated that the modified honeybee toxin, TPNQ, binds to particular residues at the external mouth of Kir1.1.[16] Figure 17 is a model of 2 adjacent subunits of R128Y-Kir1.1b in the membrane spanning region. An aromatic residue at the outer region of the channel F129-Kir1.1b (F148-Kir1.1a) has been identified as critical for TPNQ binding and block.[16] In addition, the H12 residue of TPNQ was implicated in the pH dependent binding of this toxin to wt-Kir1.1.[24]

Our studies indicate that at any given pH, R128Y had a lower affinity for TPNQ block than wt-Kir1.1, with the K_D averaging 2 orders of magnitude higher in R128Y. This would be consistent with the bulky *Tyr* side-chain of R128Y (cyan) impeding the close approach of TPNQ to the outer mouth of the mutant channel.

Methods

Mutant construction & expression of channels

Point mutations in Kir1.1b (ROMK2; EMBL/GenBank/DDBJ accession No. L29403) were engineered with a PCR QuickChange mutagenesis kit (Stratagene), using primers synthesized by Integrated Data Technologies (IDT, 1710 Commercial Park, Coralville, IA 52241). Nucleotide sequences were checked on an Applied Biosystems 3100 DNA sequencing machine at the University of Chicago Cancer Research Center.

Plasmids were linearized with Not I restriction enzyme and transcribed in vitro with T7 RNA polymerase in the presence of the GpppG cap using mMESSAGE mMACHINE kit (Ambion, Austin, TX). Synthetic cRNA was dissolved in water and stored at -70°C before use. Stage V-VI oocytes were obtained by partial ovariectomy of female *Xenopus laevis* (NASCO, Ft. Atkinson, WI), anesthetized with tricaine methanesulfonate (1.5 g/L, adjusted to pH 7.0). Oocytes were defolliculated by incubation (on a Vari-Mix rocker) in Ca-free modified Barth's solution (82.5 mM NaCl, 2 mM KCl, 1 mM $MgCl_2$ and 5 mM HEPES, adjusted to pH 7.5 with NaOH) containing 2 mg/ml collagenase type IA (Cat# C9891, Sigma Chemical, St. Louis, MO) for 90 min, and (if necessary) another 90 min in a fresh enzyme solution at 23°C. Oocytes were injected with 5 to 10 ng of cRNA and incubated at 19°C in $2\times$ diluted Leibovitz medium (Life Technologies, Grand Island, NY) for 1 to 3 days before measurements were made.

Whole-cell experiments

Whole-cell currents and conductances were measured in intact oocytes using a two-electrode voltage clamp (Model CA-1, Dagan Corp., Minneapolis, MN) with 16 command pulses of 30 ms duration between minus 200 mV and plus 100 mV, centered around the resting potential.

Oocytes expressing Kir1.1 or mutants of Kir1.1 were bathed in permeant acetate buffers to control their internal pH as previously described.[9] The relation between intracellular and extracellular pH was calculated from a previous calibration with Kir1.1 oocytes: pHi = 0.595 × pHo + 2.4. There was no external pH dependence of single-channel conductance or gating for the channels used in this study, as determined in separate experiments with impermeant external buffers.

The bath consisted of either: 100 mM K, Rb, Tl, NH_4 or Cs; with half the cation concentration obtained from chloride salts and half from membrane permeant acetate, which insured a consistent intracellular pH. The bath also contained 1 mM $MgCL_2$, 2 mM $CaCl_2$ and 5 mM HEPES. None of the oocytes in these experiments had significant chloride currents. TPNQ (Tertiapin-Q trifluoroacetate salt) was obtained from Sigma-Aldrich (#T1567).

The external bath surrounding the oocyte could be 90% exchanged within 10 sec as determined by membrane depolarization during external K elevation.[10] All experiments described were conducted at room temperature (21 ± 2°C) on Kir1.1b (ROMK2), or mutants of Kir1.1b, expressed in Xenopus oocytes. Whole-cell conductances were normalized to the maximum whole-cell conductance for that oocyte to compensate for differences in expression efficiency between wild-type and mutant channels.

The permeability ratio P_K/P_{Na} was determined by fitting a form of the GHK equation; e.g.,

$$V_{rev} = +(RT/F)Ln[\{(P_K/P_{Na})[K]_{out} + 100 \ mM - [K]_{out}\}/b] \tag{1}$$

where extracellular $[Na]_{out}$ was progressively replaced by $[K]_{out}$ at constant ionic strength ($[Na]_{out} + [K]_{out} = 100$ mM) and R,T,F have their usual meaning. The parameter:

$$b = (P_K/P_{Na})[K]_{in} + [Na]_{in} \tag{2}$$

is a function only of internal concentrations and is assumed to remain unchanged during rapid extracellular ionic replacements. Similar equations were used for fitting the permeability ratios: P_{Rb}/P_{Na}, P_{Tl}/P_{Na} and P_{NH4}/P_{Na} during replacement of Na by Rb, Tl and NH$_4$ at constant ionic strength. Comparison of permeability ratios was facilitated by expressing all ratios relative to P_K where X denotes Rb, Tl or NH$_4$:

$$(P_X/P_K) = (P_X/P_{Na})/(P_K/P_{Na}) \tag{3}$$

Permeation of both Rb and K through R128Y was modeled as competitive enzyme inhibition with mixed alternative substrates. Our simplifying assumption is that the channel behaves similarly to an enzyme and that permeation of Rb and K through a channel is analogous to a single enzyme with 2 different substrates. Consequently, total conductance in the presence of both Rb and K is analogous to the overall velocity of the enzyme reaction, which is the sum of velocities for each substrate, assuming that each is competitively inhibited by the other.

$$G_{tot} = G_{K \ max}/[1 + (K_K/[K]) \cdot (1 + \{[Rb]/K_{Rb}\})] + G_{Rb \ max}/[1 + (K_{Rb}/[Rb]) \cdot (1 + \{[K]/K_K\})] \tag{4}$$

where G_{Kmax}, G_{Rbmax} are the maximum conductances and K_K, K_{Rb} are the Michaelis constants with only K present or only Rb present, respectively. G_{tot} was normalized to the maximal conductance at each external [K], for an external Rb concentration of 200 mM.

Single channel methods

Endogenous oocyte mechanosensitive channels were effectively eliminated from patch-clamp recordings by adding 0.5 mM LaCl$_3$ to the patch pipette. LaCl$_3$ stock solutions were prepared daily since LaCl$_3$ precipitation can occur with solutions left at room temperature for several days. In control experiments, there was no effect of LaCl$_3$ on Kir1.1 conductance or kinetics. Pipette solutions consisted of 100 mM K, Rb, Tl, NH$_4$ or Cs as chloride salts plus 2 mM CaCl$_2$, and 5 mM HEPES, with zero Mg, since Mg decreases single channel conductance.[11]

For cell-attached patches, the bath contained 10 mM KCl, 50 mM NaCl, 50 mM NaAcetate, 0 Mg, 2 mM Ca, 5 mM HEPES. The actual potential across the cell-attached patch was determined by correcting the applied pipette holding potential by the average oocyte potential, measured on the same batch of oocytes with the same outside solution, using the two-electrode voltage clamp. For excised (inside-out) patch measurements, the bath (intracellular) solution consisted of 100 mM RbCl, 0 Mg, 0 Ca and 4 mM NaF (to inhibit rundown).

Kinetic analysis of R128Y-Kir1.1b was done only on patches containing a single channel. For comparison, wild-type Kir1.1 kinetic parameters were taken from previously determined cell-attached experiments on single-channel patches in similar solutions.[11,12] Since EDTA was not used in the present experiments, we cannot exclude a contribution of trace amounts of divalents (e.g., Ba) to the longer closed state of R128Y channels. However, this type of divalent block should be similar for both R128Y and wt-Kir1.1.

Homology modeling

To facilitate interpretation of the electrophysiological results, we constructed a homology-based model of Kir1.1b. The closed-state 3.1 Å crystal structure of the chicken inward rectifier Kir2.2 (3JYC)[13] was used as the template. Modeling was done with Molecular Operating Environment (MOE), version 2009.10 (Chemical Computing Group, Montreal). The initial sequence alignment was checked manually to ensure that insertions and deletions were confined to surface residues. A series of intermediate models were generated and refined by energy minimization. The quality of the final model was checked with the MOE implementation of PROCHECK.[14]

Conclusions

A single point *Tyr* mutation at a highly conserved *Arg* (R128-Kir1.1b) in the P-loop near the selectivity filter of Kir1.1 increased the Rb/K conductance ratio (G_{Rb}/G_K) by 17 ± 3 fold and the G_{Cs}/G_K by >40 fold, primarily by a selective decrease in K conductance.

We believe that this altered preference for Rb and Cs over K occurs without major structural changes to the channel protein but may involve subtle changes in the dynamics of the selectivity filter, based on the following observations.

1. Cation conductance changes occurred without substantive changes in K/Na or Rb/Na permeability ratios.

2. There was no evidence of altered single-channel rectification, and changes in kinetics were relatively minor.

3. There were no changes in Kir1.1 pH gating, although they were alterations in the K_D of toxin binding at the outer mouth of the channel.

4. The mutant channels remained sensitive to external Ba block, which presumably occurs at the innermost K binding site in the selectivity filter.[25]

Acknowledgments

References

1. Doyle DA, Morais Cabral J, Pfuetzner RA, Kuo A, Gulbis JM, Cohen SL, et al. The structure of the potassium channel: molecular basis of K$^+$ conduction and selectivity. Science. 1998; 280:69–77. [PubMed: 9525859]

2. Armstrong CM. Ionic pores, gates and gating currents. Q Rev Biophys. 1975; 7:179–210. [PubMed: 4449982]

3. Hille B. Ionic selectivity of Na and K channels of nerve membranes. Membranes. 1975; 3:255–323. [PubMed: 1202319]

4. Lockless S, Zhou M, MacKinnon R. Sructural and Thermodynamic properties of selective ion binding in a K channel. PLos Biol. 2007; 5:1079–88.

5. Noskov SY, Berneche S, Roux B. Control of ion selectivity in potassium channels by electrostatic and dynamic properties of carbonyl ligands. Nature. 2004; 431:830–4. [PubMed: 15483608]

6. Noskov SY, Roux B. Importance of hydration and dynamics on the selectivity of the KcsA and NaK channels. J Gen Physiol. 2007; 129:135–43. [PubMed: 17227917]

7. Yang J, Yu M, Jan YN, Jan LY. Stabilization of ion selectivity filter by pore loop ion pairs in an inwardly rectifying potassium channel. PNAS. 1997; 94:1568–72. [PubMed: 9037094]

8. Choi H, Heginbotham L. Functional influence of the pore helix glutamate in the KcsA K^+ channel. Biophys J. 2004; 86:2137–44. [PubMed: 15041654]

9. Choe H, Zhou H, Palmer LG, Sackin H. A conserved cytoplasmic region of ROMK modulates pH sensitivity, conductance and gating. Am J Physiol. 1997; 273:516–29.

10. Sackin H, Nanazashvili M, Li H, Palmer LG, Walters DE. External K activation of Kir1.1 depends on the pH gate. Biophysical J. 2007; 93:14–6.

11. Sackin H, Nanazashvili M, Palmer LG, Krambis M, Walters DE. Structural locus of the pH gate in the Kir1.1 inward rectifier channel. Biophys J. 2005; 88:2597–606. [PubMed: 15653740]

12. Choe H, Sackin H, Palmer LG. Gating Properties of Inward-Rectifier Potassium Channels: Effects of Permeant Ions. J Membrane Biol. 2001; 184:81–9. [PubMed: 11687881]

13. Tao X, Avalos J, Chen J, MacKinnon R. Crystal structure of the eukaryotic strong inward-rectifier K channel Kir2.2 at 3.1 Å resolution. Science. 2009; 326:1668–74. [PubMed: 20019282]

14. Laskowski RA, MacArthur MW, Moss DS, Thornton JM. PROCHECK: a program to check the stereochemical quality of protein structures. J Appl Cryst. 1993; 26:283–91.

15. Chepilko S, Zhou H, Sackin H, Palmer LG. Permeation and gating properties of a cloned renal K^+ channel. Am J Physiol. 1995; 268:389–401.

16. Jin W, Klem A, Lewis J, Lu Z. Mechanisms of inward-rectifier K channel inhibition by Tertiapin-Q. Biochemistry. 1999; 38:14294–301. [PubMed: 10572004]

17. Sackin H, Nanazashvili M, Li H, Palmer LG, Walters DE. An intersubunit salt bridge near the selectivity filter stabilizes the active state of Kir1.1. Biophys J. 2009; 97:1058–66. [PubMed: 19686653]

18. Sackin H, Syn S, Palmer LG, Choe H, Walters DE. Regulation of ROMK by extracellular cations. Biophys J. 2001; 80:683–97. [PubMed: 11159436]

19. Choe H, Sackin H, Palmer LG. Permeation and gating of an inwardly rectifying potassium channel: Evidence for a variable energy well. J Gen Physiol. 1998; 112:433–46. [PubMed: 9758862]

20. Choe H, Palmer LG, Sackin H. Structural determinants of gating in inward-rectifier K^+ channels. Biophys J. 1999; 76:1988–2003. [PubMed: 10096896]

21. Zhou H, Chepilko S, Schutt W, Choe H, Palmer LG, Sackin H. Mutations in the pore region of ROMK enhance Ba^{2+} block. Am J Physiol. 1996; 271:1949–56.

22. Eisenman G. Cation selective glass electrodes and their mode of operation. Biophys J. 1962; 2:259–323. [PubMed: 13889686]

23. Sackin H, Nanazashvili M, Palmer LG, Li H. Role of conserved glycines in pH gating of Kir1.1 (ROMK). Biophys J. 2006; 90:3582–9. [PubMed: 16533837]

24. Ramu Y, Klem A, Lu Z. Titration of Tertiapin-Q inhibition of ROMK1 channels by extracellular protons. Biochemistry. 2001; 40:3601–5. [PubMed: 11297426]

25. Jiang Y, MacKinnon R. The barium site in a potassium channel by X-ray crystallography. J Gen Physiol. 2000; 115:269–72. [PubMed: 10694255]

26. Choe H, Sackin H, Palmer LG. Permeation properties of inward-rectifier potassium channels and their molecular determinants. J Gen Physiol. 2000; 115:391–404. [PubMed: 10736307]
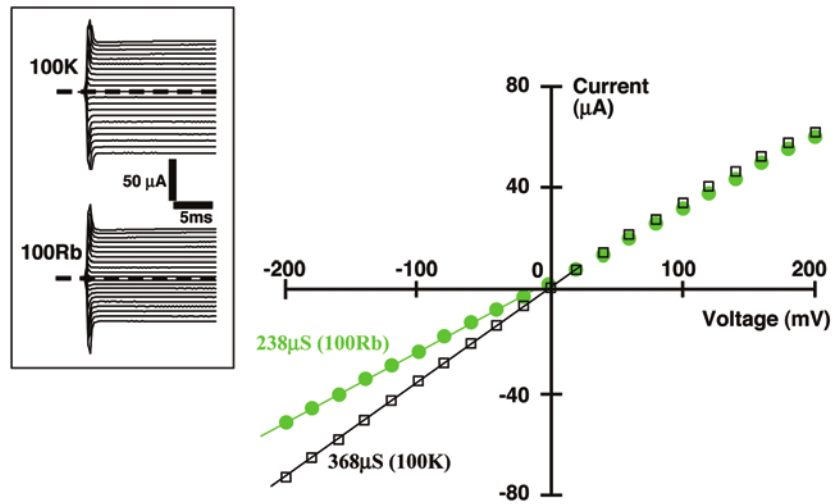
Figure 1.
Whole-cell current-voltage relations for wt-Kir1.1b, with either 100 mM extracellular K (black) or 100 mM extracellular Rb (green). Currents were measured on the same oocyte in response to applied clamp voltages between -200 mV and +200 mV. Oocyte internal [K] was approximately 100 mM and acetate buffers were used to clamp the oocyte internal pH at 7.8. Fitted lines indicate either K (black) or Rb (green) inward conductances. Inset shows raw data.
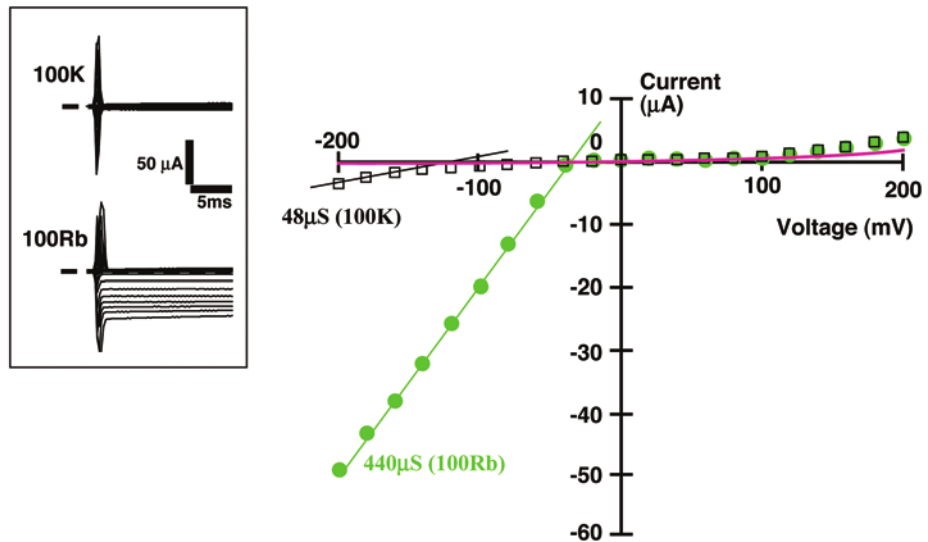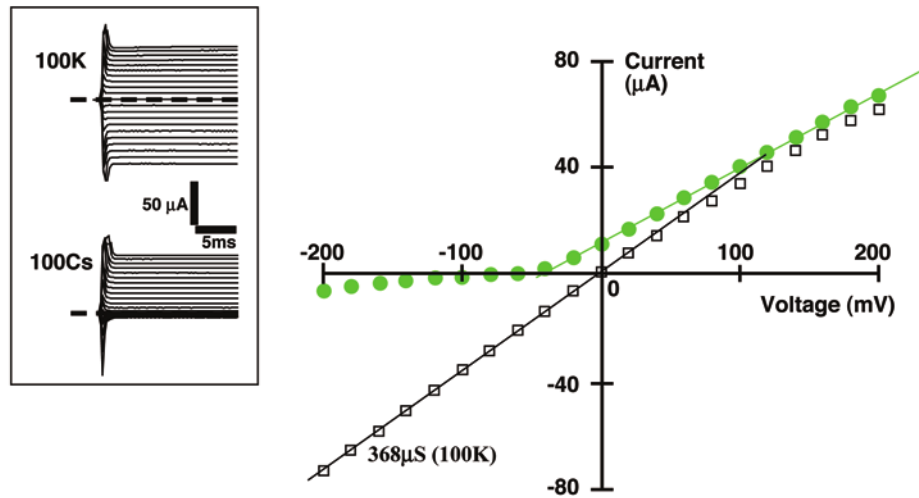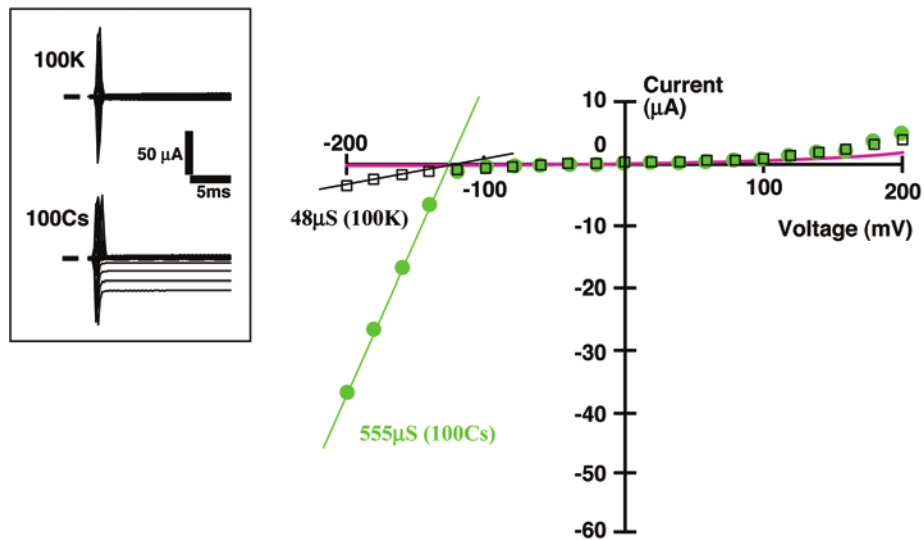
Figure 2.
Whole-cell current-voltage relations for R128Y-Kir1.1b, with either 100 mM extracellular K (black) or 100 mM extracellular Rb (green). Currents were measured on the same oocyte in response to applied clamp voltages between -200 mV and +200 mV. Oocyte internal [K] was approximately 100 mM and acetate buffers were used to clamp the oocyte internal pH at 7.8. Fitted lines indicate either K (black) or Rb (green) inward conductances. Magenta curve indicates the average I-V relation for an uninjected oocyte bathed in 100 mM external K. Inset shows raw data.

Figure 3.
Whole-cell current-voltage relations for wt-Kir1.1b, with either 100 mM extracellular K (black) or 100 mM extracellular Cs (green). Currents were measured on the same oocyte in response to applied clamp voltages between -200 mV and +200 mV. Oocyte internal [K] was approximately 100 mM and acetate buffers were used to clamp the oocyte internal pH at 7.8. Inward conductances reflect either Cs (green) or K (black) permeation. Outward conductances reflect flow of K out of the oocyte. Inset shows raw data.

Figure 4.
Whole-cell current-voltage relations for R128Y-Kir1.1b, with either 100 mM extracellular K (black) or 100 mM extracellular Cs (green). Currents were measured on the same oocyte in response to applied clamp voltages between -200 mV and +200 mV. Oocyte internal [K] was approximately 100 mM and acetate buffers were used to clamp the oocyte internal pH at 7.8. Fitted lines indicate either K (black) or Cs (green) inward conductances. Outward conductances reflect flow of K out of the oocyte. Magenta curve indicates the average I-V relation for an uninjected oocyte bathed in 100 mM external K. Inset shows raw data.
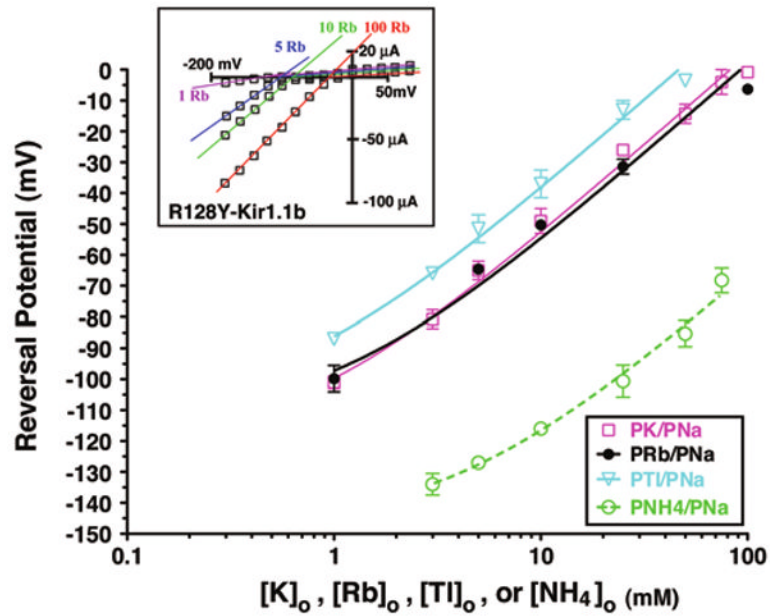
Figure 5.
Semi-log plot of R128Y reversal potentials associated with progressive replacement of external Na by: K (open squares), Rb (closed circles), Tl (open triangles) or NH$_4$ (open circles), at constant ionic strength. Permeability ratios were fit by Eqs 1–3 (Methods) and given in Table 2. Inset shows an example of R128Y inward and outward currents during isosmolar replacement of external Na by Rb.
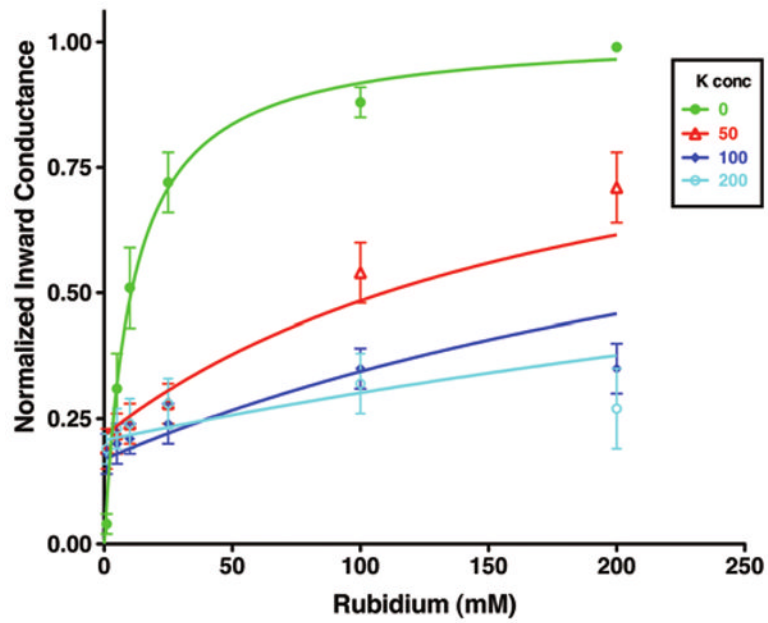
Figure 6.
External K is a competitive inhibitor of inward Rb current in R128Y. Total inward whole-cell conductance was normalized to the maximal conductance at each external [K], which occurred at an external Rb concentration of 200 mM. Curves were drawn from a competitive inhibitor model (Eq 4, Methods). Fitted parameters are given in the text.
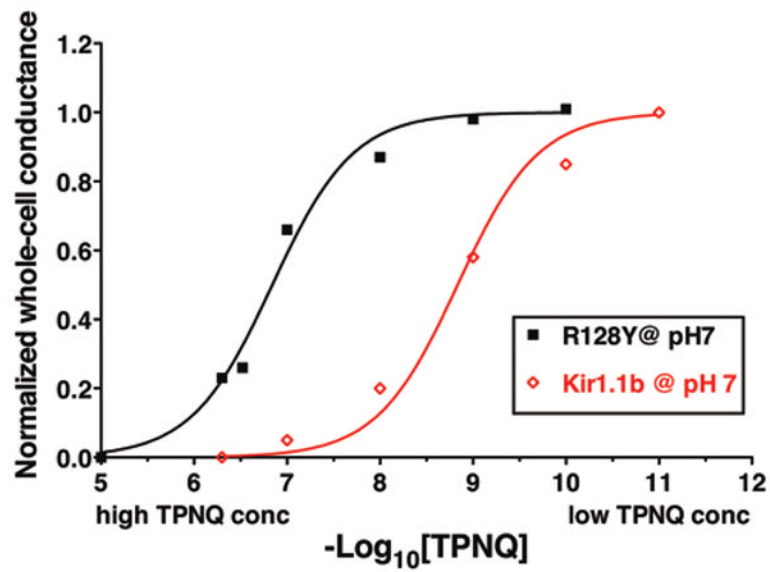
Figure 7.
Comparison of TPNQ dose-response curves for ROMK vs. R128Y. Binding and block of wt-Kir1.1 (ROMK) by TPNQ at external pH 7, $K_D = 1.5 \times 10^{-9}$ M (red, open diamonds); and binding and block of R128Y-Kir1.1b by TPNQ at external pH 7, $K_D = 1.5 \times 10^{-7}$ M (black, closed squares).
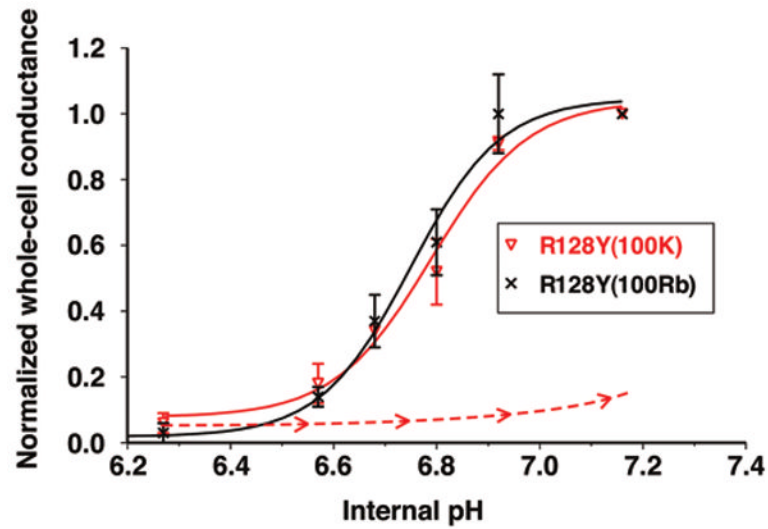
Figure 8.
Internal acidification in 100 mM Rb solutions reversibly closed R128Y with a pKa of 6.7 ± 0.03 (black). The same acidification in 100 mM external K closed R128Y with a pKa of 6.8 ± 0.03 (red), similar to the pKa of 6.7 ± 0.02 for wt-Kir1.1b. however, R128Y recovered very slowly during realkalization in 100 mM K (dashed red line).
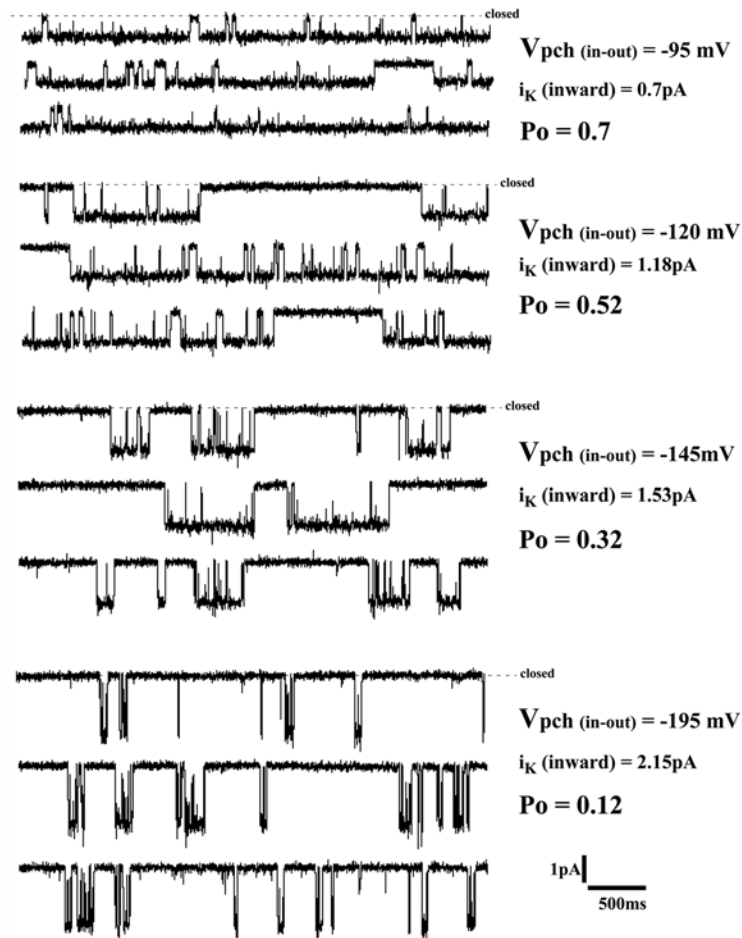
Figure 9.
Single-channel inward Rb currents through a cell-attached patch on an R128Y oocyte. The bath solution consisted of: 0 Mg, 2 mM Ca and 10 mM K, which depolarized the oocyte to -45 mV. The patch pipette contained 100 mM Rb, 0 Mg, 2 Ca, and pipette holding potentials were varied between +50 mV and +150 mV relative to the bath (ground). One R128Y channel in the patch, having inward Rb conductance of 14.2 pS. Records were sampled at 5 khz & filtered at 300 Hz.
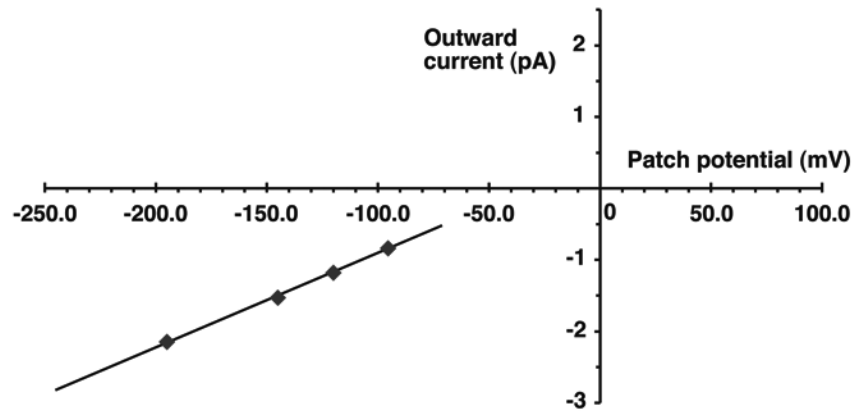
Figure 10.
Single-channel current-voltage relation showing inward Rb current but no discernable outward K current through the R128Y cell-attached patch of Figure 9. Oocyte bathed in 10 mM K, 0 Mg, 2 mM Ca, which depolarized the oocyte to -45 mV. Pipette: 100 RbCl, 0 Mg, 2 Ca, 0.5 mM LaCl$_3$. Inward single-channel Rb conductance = 14.2 pS.
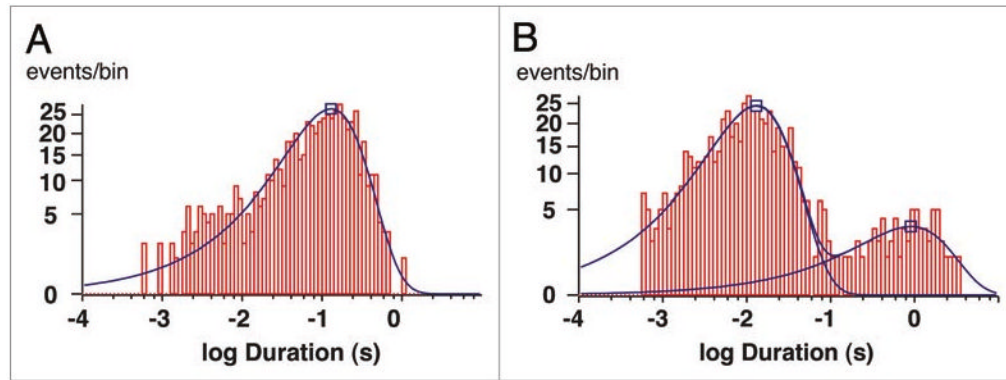
Figure 11.
Histograms for the R128Y inward Rb current of Figure 9 at a V_{pch} of -120 mV (inside negative). Oocyte was bathed in 10 mM K, 0 Mg, 2 mM Ca, which depolarized the oocyte to -45 mV. Pipette: 100 RbCl, 0 Mg, 2 Ca, 0.5 mM $LaCl_3$ at a pipette holding potential of +75 mV. (a) Mean open time = 129 ms (1,254 events, one channel). (B) Two closed states with mean closed times = 13 ms (88%) and 905 ms (12%).
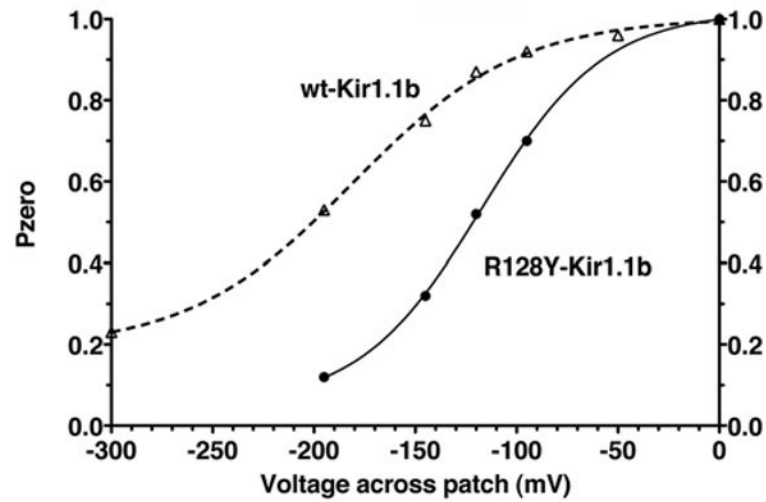
Figure 12.
Voltage dependence of open probability (Po) for the single-channel Rb current of R128Y in Figure 9, compared to wt-Kir1.1 Rb permeation (dashed line). Curve is the best fit to the Boltzman Eq: Po = Bottom + (Top - Bottom)/(1 + exp((V_{50} - V)/slope)), where V_{50} = -117 mV and slope = 30, for R128Y and V_{50} = -181 mV and slope = 41, for wild-type.
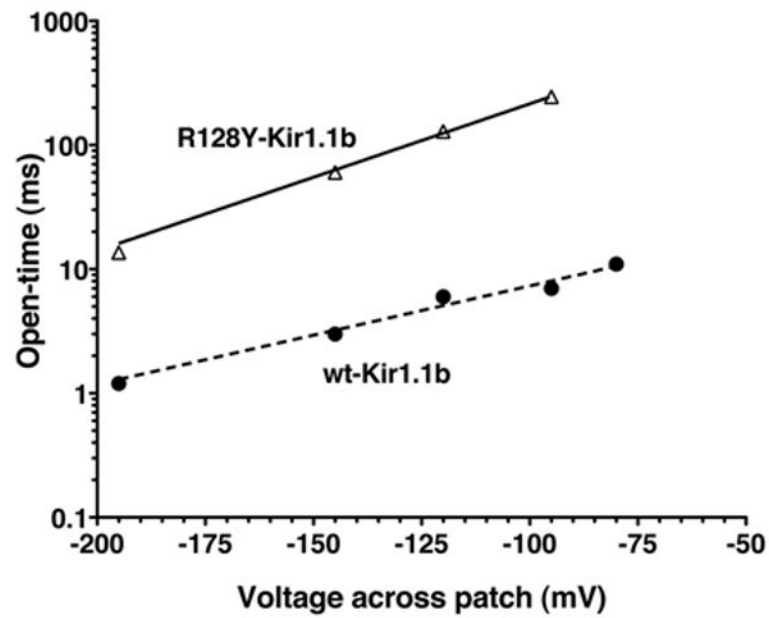
Figure 13.
Voltage dependence of mean open time for the single-channel Rb current of R128Y in Figure 9, compared to wt-Kir1.1 Rb permeation (dashed line). The data were fit to a simple exponential: Tau (open time) = α•exp(β•V), where α = 3280 for R128Y and 58 for wt, and β = 0.03 for R128Y and 0.02 for wt.
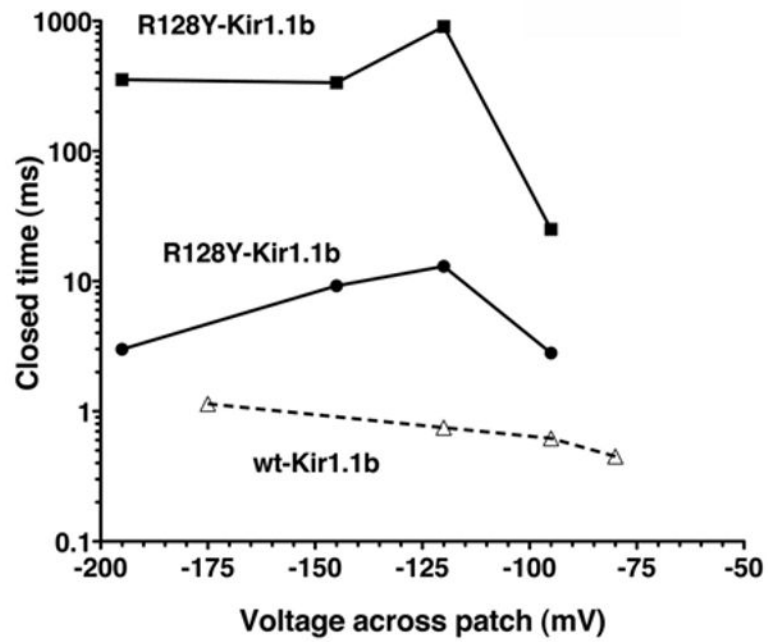
Figure 14.
Voltage dependence of the 2 closed times (squares, circles) for the single-channel R128Y Rb currents in Figure 9, compared to wt-Kir1.1 Rb currents (open triangles, dashed line), which have only a single closed state.[12]
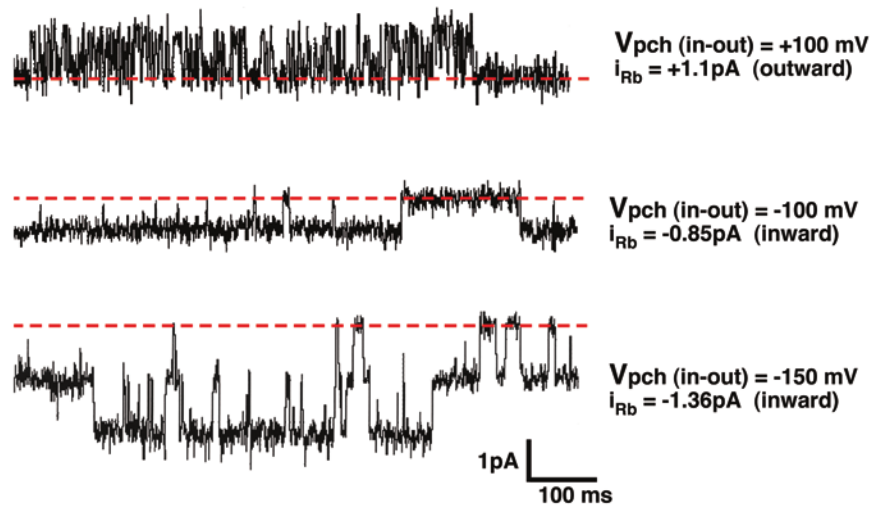
Vpch (in-out) = +100 mV
i_{Rb} = +1.1pA (outward)

Vpch (in-out) = -100 mV
i_{Rb} = -0.85pA (inward)

Vpch (in-out) = -150 mV
i_{Rb} = -1.36pA (inward)

1pA
100 ms

Figure 15.
Rb currents from an excised R128Y patch with 100 mM RbCl, zero Mg, 2 mMCa, 0.5 mM LaCl$_3$ in the pipette and 100 mMRbCl, zero Mg, zero Ca, 4 mM NaF in the bath at pH = 9. Upward deflections from the thick dashed line (closed state) correspond to outward current at V_{pch} = +100 mV (top trace). Downward deflections from the dashed line denote inward currents at V_{pch} = -100 mV and -150 mV respectively.
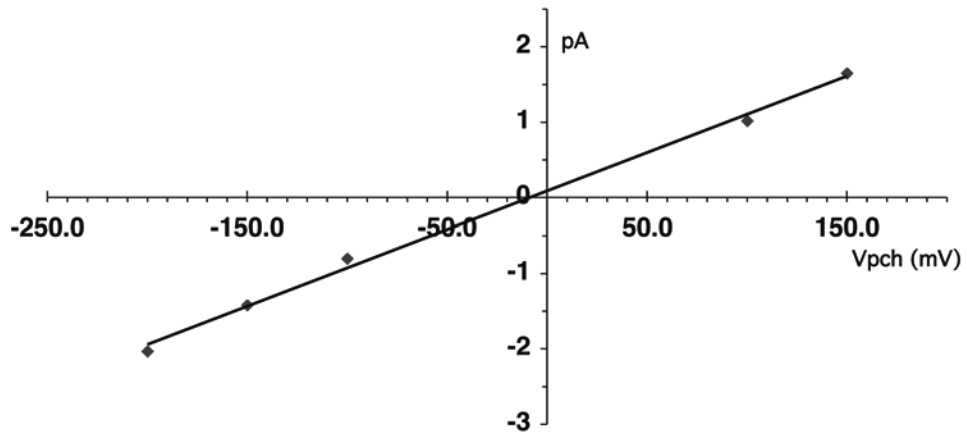
Figure 16.
Excised current-voltage relation for Rb currents through R128Y. Single channel Rb conductance was 10.2 pS. There was no obvious rectification of single-channel current in the absence of bath Mg and polyamines. Pipette: 100 mM RbCl, 0 Mg, 0 Ca, 0.5 mM LaCl₃. Bath: 100 mM RbCl, 0 Mg, 0 Ca, 4 NaF, pH 9.
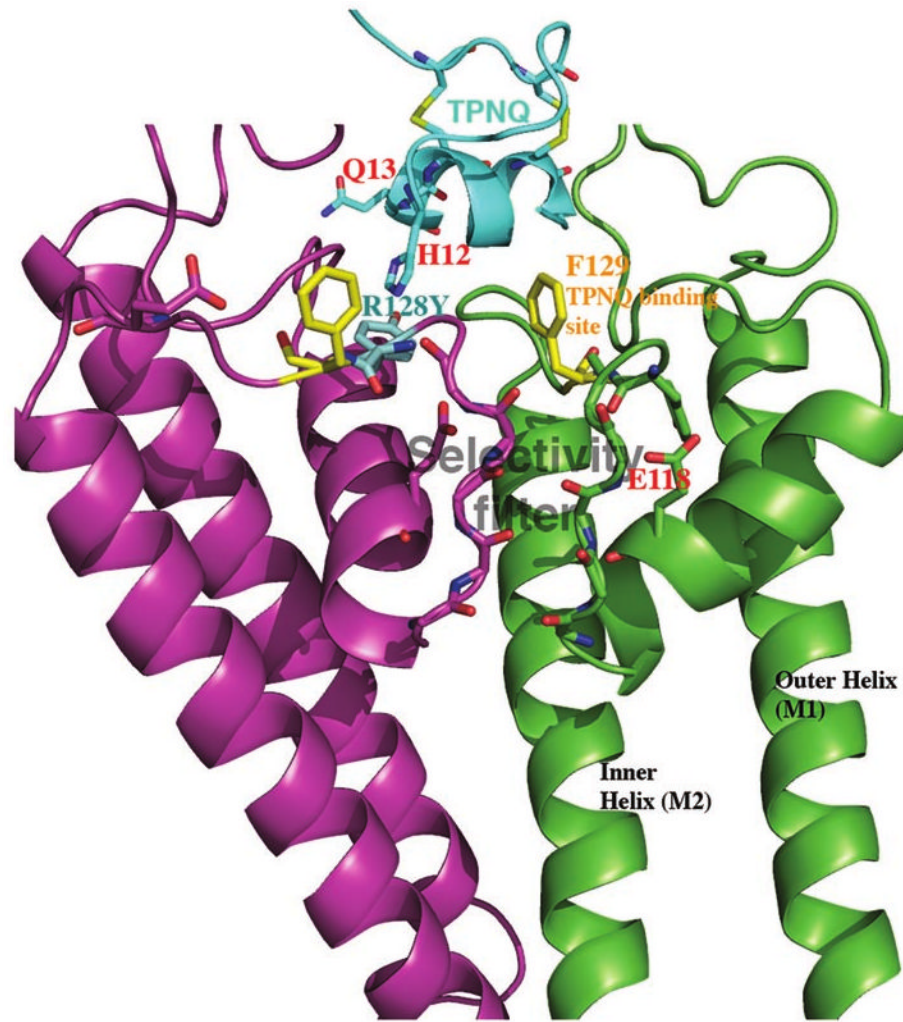
Figure 17.
The modified honeybee toxin, TPNQ (cyan), blocks wt-Kir1.1 by binding to the outer mouth of the channel at F129-Kir1.1b (yellow side chains). TPNQ also blocks the mutant channel, R128Y-Kir1.1b, but with a 100 fold higher K_D, consistent with the *Tyr* side-chain of R128Y (cyan) impeding close approach of the toxin. picture was drawn with PYMOL from our homology model, based on Kir2.2,[13] (see Methods) and the known structure of TpNQ.[16]

Table 1

Effect of a conserved P-loop *Arg* on cation selectivity

	G_{Rb}/G_K	G_{Tl}/G_K	G_{NH4}/G_K	G_{Cs}/G_K
Kir1.1b	0.7 ± 0.1 (n = 9)[*]	0.8 ± 0.1 (n = 5)[*]	0.8 ± 0.1 (n = 5)[*]	0.2 ± 0.1 (n = 5)
R128Y	11.7 ± 2 (n = 17)	2.2 ± 0.2 (n = 11)	5.1 ± 0.3 (n = 9)	8.6 ± 1 (n = 11)
R128M	3.5 ± 0.5 (n = 9)	2.6 ± 0.3 (n = 5)	5.3 ± 0.3 (n = 5)	2.2 ± 0.2 (n = 5)

Conductance ratios were measured on linear I–V plots at an oocyte potential of -60 mV, except for G_{Cs}/G_K which was determined at an oocyte potential of -180 mV.

[*] not significantly different ($p < 0.01$).

{Sackin et al.}

Table 2

Effect of a conserved P-loop *Arg* on cation permeability

	P_{Na}/P_K	P_{Rb}/P_K	P_{Tl}/P_K	P_{NH4}/P_K
Kir1.1b	0.006 ± 0.001 (n = 6)[*]	0.6 ± 0.2 (n = 13)[†]	0.9 ± 0.3 (n = 5)[§]	0.3 ± 0.1 (n = 7)[††]
R128Y	0.007 ± 0.003 (n = 8)[*]	0.6 ± 0.4 (n = 8)[†]	1.1 ± 0.5 (n = 5)[§]	0.2 ± 0.1 (n = 9)[††]
R128M	0.008 ± 0.003 (n = 4)[*]	0.6 ± 0.2 (n = 4)[†]	1.0 ± 0.4 (n = 5)[§]	0.3 ± 0.1 (n = 5)[††]

Permeability ratios were fit from reversal potential data during progressive replacement of Na by K, Rb, Tl or NH4, using Eqs (1–3).

[*] not significantly different ($p < 0.01$).

[†] not significantly different ($p < 0.01$).

[§] not significantly different ($p < 0.01$).

[††] not significantly different ($p < 0.01$).

Table 3

Effect of R128Y on single-channel conductance (pS)

	g_K	g_{Rb}	g_{Tl}	g_{NH4}	g_{Cs}
Kir1.1b	33.0 ± 1 (n = 6)	18.0 ± 2 (n = 5)*	21.0 ± 1 (n = 3)*	62.0 ± 2 (n = 3)*	-
R128Y	<1.5	12.4 ± 0.5 (n = 16)	11.1 ± 3 (n = 3)	7.7 ± 0.5 (n = 5)	11.8 ± 0.3 (n = 4)

All conductances are inward conductances, measured in cell-attached patches with zero Mg in the pipette, at 100 mM pipette cation concentrations.

*
These conductances were previously determined in our lab under similar conditions.[26]